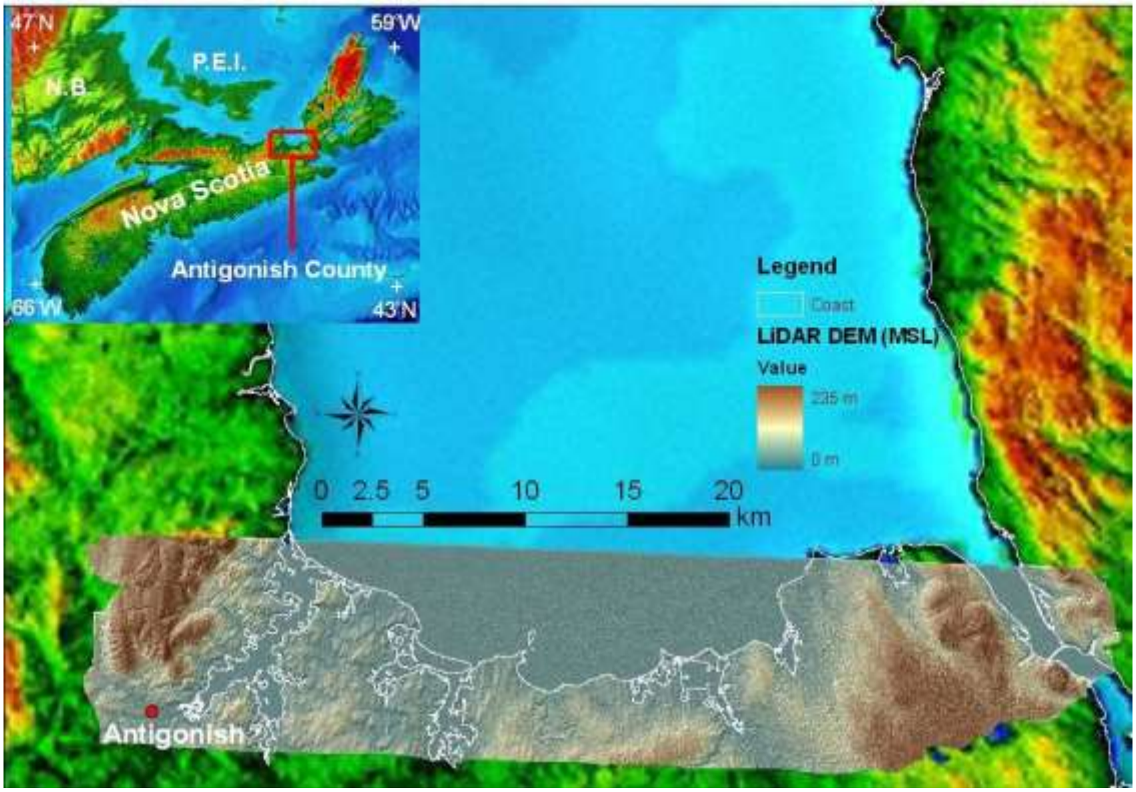

Antigonish Floodrisk and Erosion Climate Change Project

The study commissioned by the

Nova Scotia Department of Regional Economic Development and

the Nova Scotia Department of the Environment

By

Dr. Tim Webster, Katie LeBlanc and Nathan Crowell

Applied Geomatics Research Group,

Centre of Geographic Science

Nova Scotia Community College

Middleton, NS B0S 1M0

& Acadia University, Wolfville, NS

Executive Summary

The Canadian coastlines have been assessed for sensitivity to future sea-level change and it has been determined that the east coast of Canada is highly vulnerable to erosion and flooding. The third assessment of the Intergovernmental Panel on Climate Change (IPCC) indicates that there will be an increase in mean global sea-level from 1990 to 2100 between 0.09 m and 0.88 m (Church et al. 2001). The latest IPCC Assessment Report 4 (AR4) has projected global mean seal-level to rise between 0.18 and 0.59 m from 1990 to 2095 (Meehl et al. 2007). However as Forbes et al. (2009) point out, these projections do not account for the large ice sheets melting and measurements of actual global sea-level rise are higher than the previous predictions of the third assessment report. Rhamstorf et al. (2007) compared observed global sea-level rise to that projected in the third assessment report and found it exceeded the projections and have suggested a rise between 0.5 and 1.4 m from 1990 to 2100. Thus, Forbes et al. (2009) use the upper limit of 1.3 m as a precautionary approach to sea-level rise projections in the Halifax region. The selection of an upper limit of flooding is dependent on realistic projections of sea-level rise, thus because of the variations in projections we have generated flood risk maps to the 5 m contour level. This method ensures GIS layers that can be used as projections of sea-level change in the future. A Large section of the Antigonish County coastline was mapped using airborne LiDAR (Light Detection and Ranging) to construct 1 m grid cell elevation models with vertical accuracies better than 30 cm. The LiDAR was used in addition to water level records from the Pictou tide gauge to construct flood inundation maps for storm surge events and projected sea-level rise from climate change up to the 5 m contour. Return periods (e.g. 1 in 100 year event) and probability of occurrence for water levels were calculated using the tide gauge time series from Pictou. The GIS mapping provides the inundation limit of a given water level

and the associated risk is determined from the return period of that event. Under current sea-level rise conditions (32 cm/century) the 50-year return period water level is 1.95 m above mean sea level and the 100-year return period is 2.22 m. However, by incorporating a modest projection of future sea-level rise conditions, these increase to 2.1 m and 2.5 m respectively. The scientific literature describes many climate change scenarios resulting in a wide range of possible global sea-level rise predictions. We have chosen a median value of 0.5 m/century, as has been used in previous climate change flood risk projects (PEI and NB), and use this to project increased sea-levels. However, GIS flood layers have been constructed every 10 cm up to the 5 m contour, so any projected flood level using any rate can be extracted and mapped. In addition to global sea level, the relative sea level is affected by the vertical motion of the earth's crust. In this region it is estimated to be sinking at 20 cm/century, thus resulting in 0.7 m of relative sea-level rise over the next century.

In addition to flood risk mapping, this project also addresses erosion risk along the same coastline. Prior to Utting and Gallacher (2009), which is part of this initiative, there has not been any detailed examination of erosion along this shoreline. Shaw et al. 1998 report on erosion rates of 20-40 cm per year west of the study area in the River John area. In order to assess the past changes in the coastline a series of historical aerial photographs have been scanned, orthorectified (geocoded) and used in a GIS to interpret the shoreline position. Photos from 1954, 64, 71, 79, 90, 97, 07 were scanned, rectified and shorelines interpreted. From the different shorelines, rates of erosion or accretion were calculated at select locations. Several segments of this section of coastline are protected from development by the Department of Natural Resources. As a result there are no artificial protective structures (armour stone, riprap, groins, breakwaters, etc.). This is in contrast to the privately owned armoured shoreline north of Antigonish. The erosion of the shoreline is strongly controlled by the geological material that forms the shoreline. As a result the headland promontories are often comprised of bedrock and forms cliffs several metres high. Glacial till in drumlins form the other dominant shoreline material and form slumped or steep embankments several metres high. The embayments are comprised of dune systems and lagoons. Dunns Beach was studied in detail because of the active slumping of the glacial till embankment. The shoreline is comprised of a series of actively eroding drumlins orientated perpendicular to the coast. The rates of erosion are between 20 and 60 cm per year or 1-2 feet per year. Cape Jack was also examined in detail because of the close proximity of a critical rail line that connects Cape Breton and the mainland. The rail bed is exposed in culvert locations where the thin 2-4 m high glacial till bank has eroded. The till bank is eroding at a rate of 20 cm per year (~ 1 foot), while the adjacent shoreline at a lower elevation has retreated into a pond at a rate of 70 cm per year (over 2 feet). In contrast to these eroding shorelines, the Pomquet dune systems is growing and accumulating land at a rate between 50 and 150 cm per year (2 – 5 feet).

Table of Contents

List of Figures

List of Tables

1. Introduction

Global climate is changing due to the increase of greenhouse gas emissions, the resulting warming trends may result in an observed increase of global sea levels (Titus et al. 1991). Future projections of sea-level change depend on estimated future greenhouse gas emissions and are predicted based on a number of scenarios (Raper et al. 2006). Based on projections from the third assessment of the Intergovernmental Panel on Climate Change (IPCC), global mean sea level will increase between 0.09 m and 0.88 m with a central value of 0.5 m between the years 1990 and 2100 (Webster & Forbes, 2005). The main contributions to global mean sea level will be due to thermal expansion of the oceans (0.11 – 0.43 m), melting of glaciers (0.01 to 0.23 m)and ice sheets in Greenland (-0.02 to 0.09 m), and Antarctica (-0.17 to 0.02 m) (Church et al. 2001). The latest IPCC Assessment Report 4 (AR4) has global mean seal-level projected to rise between 0.18 and 0.59 m from 1990 to 2095. However, as Forbes et al. (2009) point out, these projections do not account for the large ice sheets and have predicted the measurements of actual global sea-level rise to be higher than the previous predictions of the third assessment report. Rhamstorf et al. (2007) compared observed global sea-level rise and found it exceeded the projections of the third IPCC report and have suggested a rise between 0.5 and 1.4 m from 1990 to 2100. This projected increase in global mean sea level and the fact that many coastal areas of Maritime Canada have been deemed highly susceptible to sea-level rise (Shaw et al. 1998) has lead to the initiation of various studies to produce detailed flood-risk maps of coastal communities in PEI, NB, and NS (Webster et al. 2004; Webster and Forbes, 2005; Webster et al. 2006; Webster et al. 2008).

The purpose of this project was to look at the extent and impact of various flood levels for the Antigonish County coastline (Fig. 1) and assign return periods for present day and future sea-level rise conditions from climate change. In addition, an analysis of past erosion rates was calculated for this shoreline based on historical aerial photographs. A Previous regional study by Nicol (2206) highlighted the requirement high resolution mapping of the shoreline in order to produce useful flood risk maps and that no previous detailed erosions studies have been completed for this area. LiDAR (Light Detection and Ranging) ‘ground’ hits were used to construct a Digital Elevation Model (DEM) as the basis for the production of flood-risk maps and Water Modeler has been used to determine return periods of various flood levels. This project has been funded by the Nova Scotia Department of the Environment, the Nova Scotia Department of Economic Development, and the Nova Scotia Department of Natural Resources. Flood-risk mapping studies in the Maritime Provinces have been carried out by Webster and Forbes (2005), Webster et al. (2006), and Webster et al. (2008) and were the basis for the methodology employed in this study. In these past studies, return periods of high water levels were provided by Dalhousie Department of Oceanography. Bernier (2005) used 40 years of tide gauge records for the region and 40 years of wind observations to drive the Dalhousie storm surge model and compared return period of storm surges and total water level. Bernier and Thompson (2006) and Thompson et al. (2009) present results of the extreme sea levels for the Atlantic Canada region. In this study we utilized a new program, Water Modeler that analyzes a time-series of water levels from tide gauge records to calculate return periods (Webster et al. 2008).

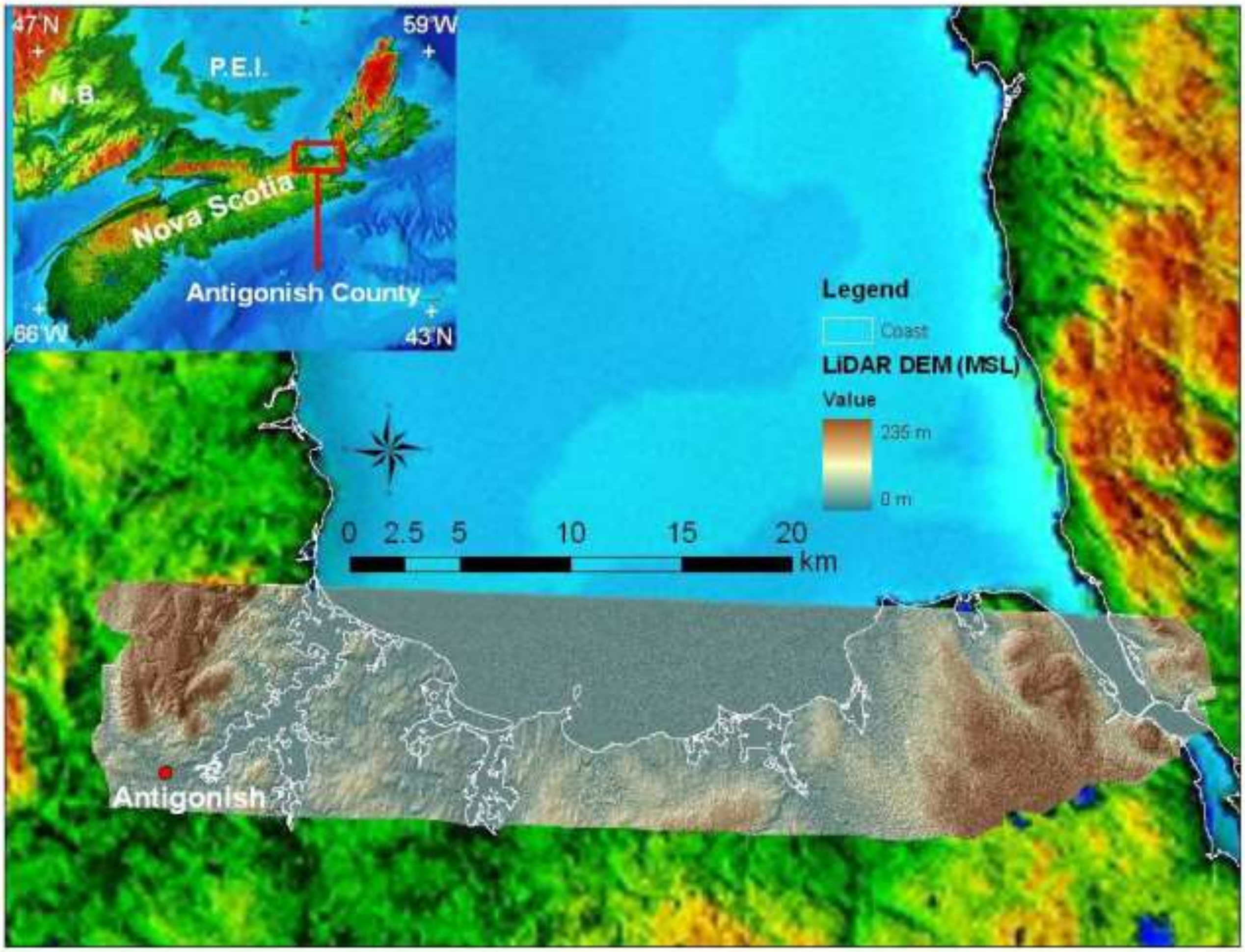

Figure 1: Overview of study area with the LIDAR DEM overlaid along the Antigonish County coastline. The inset map shows the study area location within Maritime Canada.

2. Methods

2.1 LiDAR

Airborne LiDAR is a useful remote sensing technology that is used to acquire information about the Earth's surface. A LiDAR system is composed of three technologies: GPS (Global Positioning System); an IMU (Inertial Measurement Unit); and a laser ranging system (Flood & Gutelius, 1997; Liu, 2008). The GPS was used to determine the geographic position and elevation of the aircraft. The IMU was used to measure the attitude of the aircraft (roll, pitch and heading; Liu, 2008). The roll, pitch, and heading were accurately measured to allow for the correction of the motion of the aircraft by computer software (Flood & Gutelius, 1997). The laser ranging system transmitted a laser pulse towards the Earth's surface in a wide swath, and recorded the time delay between the transmission of the laser pulse and its return. Each laser pulse was capable of recording up to four returns encoded with the GPS, IMU and range data (Liu, 2008). Researchers such as Flood & Gutelius (1997) and Wehr & Lohr (1999) provide a general description and overview concerning airborne LiDAR technology and the principles behind it.

LiDAR was flown on November 17th and December 8, 2008 over the Antigonish coastline by the Applied Geomatics Research Group (AGRG), Middleton, Nova Scotia, Canada. The Optec ALTM 3100 LiDAR platform collected first and last returns at a repetition rate of 70 kHz, a scan frequency of 38 Hz, and a scan angle of 24^{o}. Flight lines were surveyed with a 50% overlap. The survey achieved an average a point spacing of every 0.5 m.

2.1.1 LiDAR Processing

After the flights the GPS and IMU data were processed to determine the trajectory of the aircraft. Once this was done, the laser scans were linked via a GPS time tag to the trajectory and the LiDAR point clouds were exported as binary LAS format files per flight line. These files were large and contained billions of points and were required to be processed in specialized LiDAR software from Terrascan™. A Terrascan project was defined that had 592 blocks which measured 1040 m by 1040 m. Blocks were used to process the data in more manageable file sizes (Fig. 2).

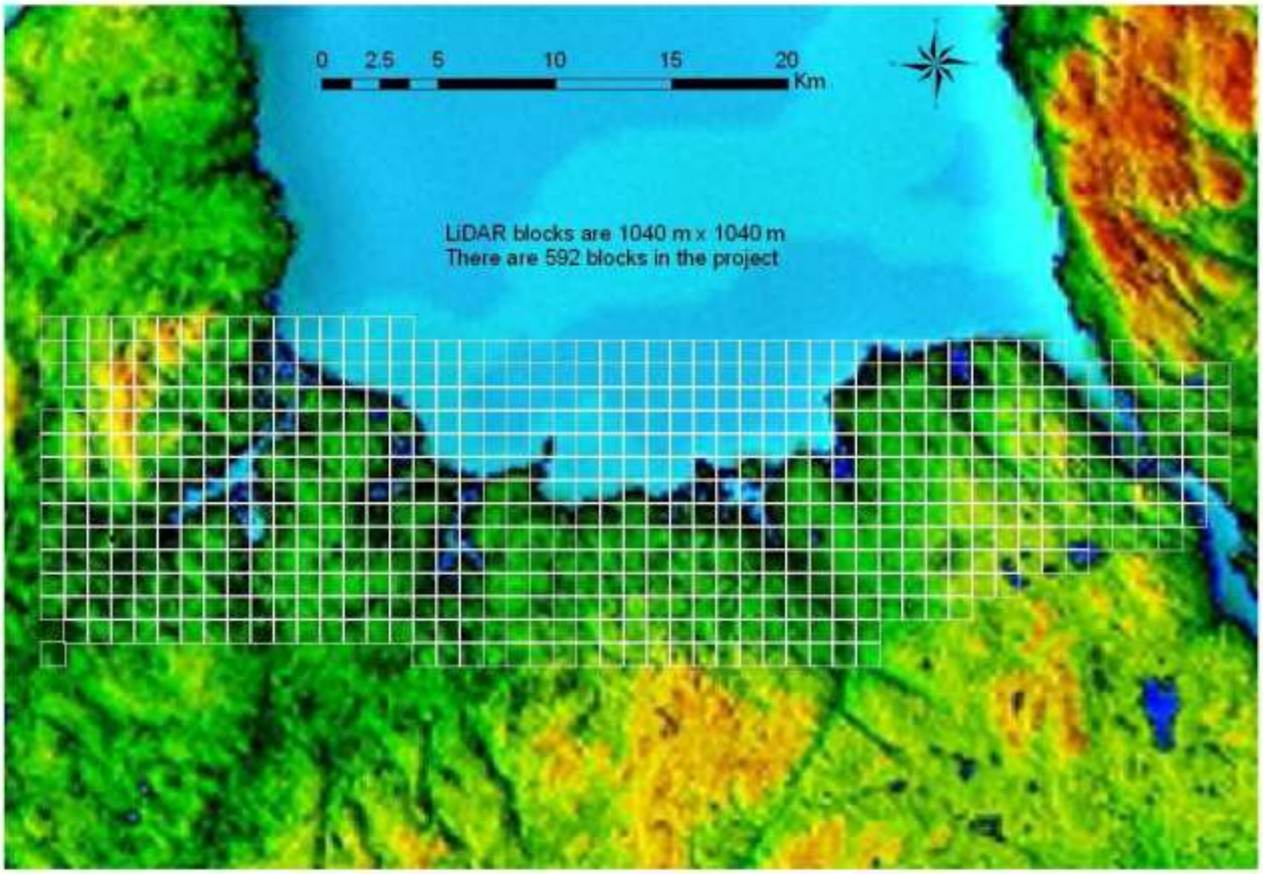

Figure 2 Blocks used to process the LiDAR data, each block is 1040 m by 1040 m.

Upon visual inspection of the LiDAR flight lines differences in the spatial locations of common features between flight lines were observed. Offsets included both horizontal and vertical shifts of features (Fig. 3). These problems were indicative of poor calibration results which relate the GPS, IMU, LiDAR sensor to the axis of the aircraft. Although the calibration numbers reported errors within specifications, the offsets within the flight lines needed to be resolved.

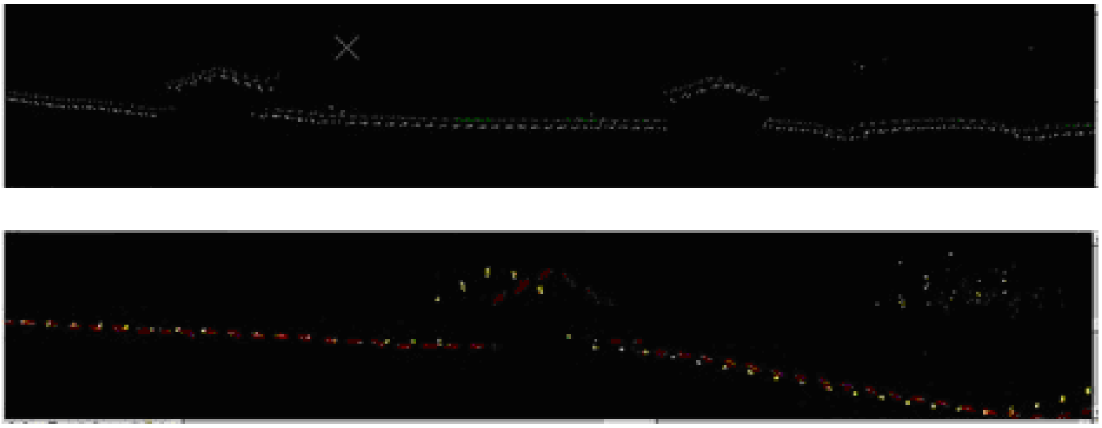

Figure 3 Offsets between flight lines. Top image slight vertical offset between lines. Bottom image shows horizontal offset between flight lines.

The weather condition on December 2008 made the flight quite turbulent and this was considered to contribute to the problem. TerraMatch is a software program designed to empirically estimate adjustments required to bulk adjust flight lines in order to promote better matches. The software was used to analyze the data in order to attempt to resolve the offset problems. This was a very time consuming process and involved computer processes that took days to run, often producing unsatisfactory results. Other LiDAR datasets had similar offset issues and recently it was determined that a heading parameter to align the IMU with the sensor and aircraft was incorrect after the system came back from the manufacturer for maintenance. The flight lines were reprocessed using a starboard heading rotation of 0.18 degrees (Fig. 4). The adjustment greatly reduced the offset issues and some minor vertical adjustments were applied to produce a consistent set of flight lines. Each block was then processed to classify ground from non-ground returns in order to generate a digital elevation model (DEM) for flood inundation mapping. An automated approach was applied that had a set of parameters to evaluate the point cloud and classify ground. However, natural coastal landscapes can have steep vertical features that are prone to misclassification. Since the DEM will be used to simulate the real world terrain for coastal flood inundation mapping, it is critical that it be as accurate as possible along the coastline. The LiDAR point cloud was visually inspected as a series of cross-sections along the entire length of coastline. Points that were misclassified were manually corrected to be included in the ground class.

Figure 4 Flight lines after heading shift and Z adjustment applied.

Once the ground classification was assessed and deemed acceptable, surface models were constructed from the LiDAR blocks. Two surface models were constructed, a DEM which was based only on classified ground points, and a digital surface model (DSM) which incorporated all points. Point measurements produced from LiDAR contained elevations above the GRS80 ellipsoid. Most land-based topographic maps contain elevations relative to a geodetic vertical datum. In Canada, this is known as the Canadian Geodetic Vertical Datum of 1928 (CGVD28). In order to have height measurements related to sea level, an adjustment needed to be made for the local vertical separation between the ellipsoid and the geoid. This was done using the HT2 geoid model and is described in Webster et al. 2004, 2006, 2008. The DEM and DSM were converted from heights above the ellipsoid to orthometric heights above the geoid (CGVD28).

To ensure that the LIDAR DEM had accurate elevation values, the DEM was compared to RTK (real time kinematic) GPS surveys along roads. Two surveys of the Antigonish region were carried out. The first survey was done in December 2008 and the second survey in September 2009. Both surveys consisted of setting up a base station and radio over an HPN (high precision network) and then setting a rover up on a vehicle. The RTK GPS points were collected from a moving vehicle along the roads. Elevations were transformed from ellipsoidal to orthometric and compared to the LiDAR DEM following procedures outlined by Webster (2005).

The last processing step required for the DEM prior to flood inundation mapping was to ensure hydraulic connectivity along water ways. Roads that have streams running under them usually contain a culvert or bridge to allow for the flow of water. However, LiDAR point elevations only detect the surface of the road. Therefore, when determining the flow path of water to or from the ocean along low lying areas, the road represented by the unedited DEM would act as a dam or barrier. To ensure that low-lying areas are properly flooded and that they are connected to the ocean, the DEM was modified in areas of culverts or bridges to allow for hydraulic connection. We follow a similar method as outlined in Webster et al. (2006) for this procedure.

2.2 Flood Inundation Mapping

Observed hourly water levels from 1970 to 1996 for the Pictou tide gauge were obtained from the MEDS[1] (Marine Environmental Data Service) website and predicted hourly water levels were obtained from the internet TBONE[2] (tide/current predictor) website. Water levels received from tide gauges are referenced to chart datum, which is roughly equivalent to the lowest astronomical tide and varies depending on the coastal region (Webster et al. 2004). To reference these water levels to CGVD28, a calculation was performed by applying the offset between CD and CGVD28. This offset was determined to be 0.9 m for Pictou (MacCaulay, personnel communication 2009).

[1] *Marine Environmental Data Service*. Retrieved from http://www.sciencecentral.com/site/503092
[2] *TBONE*. Retrieved from tide and current predictor: http://tbone.biol.sc.edu/tide/

Flood-risk maps were generated in the ArcGIS ArcMap™ environment using an Arc script developed by the AGRG (Webster and Stiff, 2008). The script generated flood levels from 0 – 5 m above CGVD28 at 0.1 m increments while ensuring only areas connected to the ocean were flooded. Five water levels were chosen to discuss in this report: (1) the 50-year return period water level under current sea-level rise conditions; (2) the 100-year return period water level under current sea-level rise conditions; (3) a benchmark storm that occurred on December 30, 1993; (4) the December 1993 storm with 50 years of projected sea-level rise conditions from climate change; (5) the December 1993 storm with 100 years of projected sea-level rise conditions from climate change. The high water level that was used for the storm event on December 30, 1993 was 2.27 m referenced to CGVD28 (3.17 m CD). The storm surge associated with this event was 1.53 m (Fig. 5).

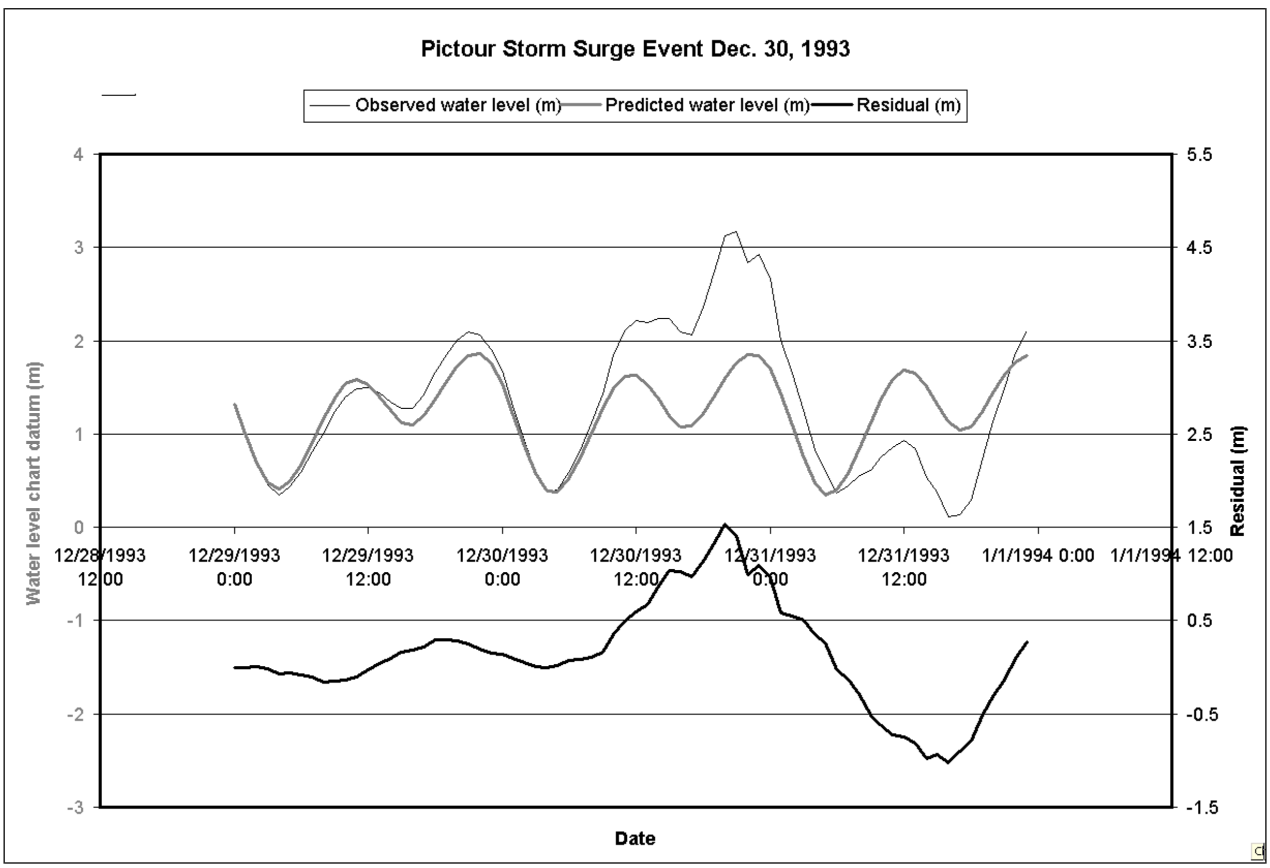

Figure 5 Observed and predicted water level for Dec 1993. Residual storm surge on right axis.

GIS and the LiDAR DEM were used to construct the flood inundation maps. To determine the risk or probability of a given water level occurring, a new software tool, Water Modeler was used. Water Modeler uses a time series of water level records (tide gauge data) to determine the risk associated with a water level (Webster et al. 2008). The return period of a given water level or the probability of occurrence can be calculated under using current sea-level rise conditions or one can use projected sea-level rise conditions predicted from climate change. A value of 32 cm/century was determined to be the current sea-level rise rate and a value of 70 cm/century was used to represent sea-level rise from climate change. The value of 70 cm/century is the same value used in the PEI study (Webster et al. 2004) and represents a combination of several factors including future global mean sea-level rise and crustal subsidence. A value of 50 cm was used to represent global mean sea-level rise and 20 cm to represent crustal subsidence. Recent work by Forbes et al. (2009) show long term GPS measurements for Halifax indicate crustal subsidence on the order of 16 cm/century. As Forbes et al. (2009) point out, several extreme water levels could be chosen and several scenarios developed for climate change, however it is the policy makers who decide what to implement. For this reason we have generated flood maps at 10 cm increments in order to account for all scenarios.

2.3 Historic aerial photography analysis and interpretation

To establish historical rates of coastline erosion and accretion, coastline positions were delineated based on a collection of orthorectified aerial photography (n = 111). The photos were obtained from the NSDNR office in the form of hardcopy prints. The photos were scanned to a 1 m ground pixel resolution. PCI Orthoengine was used to orthorectify the photos in order remove terrain displacement and establish uniform scale. . Terrain elevation data used in this process were collected from the established LiDAR DEM. A series of digital orthophotos at 20 cm resolution was obtained from the NSDNR Forestry GIS group, with restricted distribution rights. This series was used as the basis of control point selection in order to ensure older photos matched up with these most recent.

Once the photos were orthorectified, and the coastline interpreted and digitized, a broad analysis of coastline change focused on average rates of erosion between 1971 and 2007. Historical changes were assessed by delineating coastline vectors based on the observed coastline position within orthorectified aerial photography (n = 111). These rates were found to range widely due to the highly variable composition of bedrock and surficial geology throughout the coastal area.

Three unique areas of the Antigonish coastline were selected for detailed analysis using the entire temporal range of photos (Fig. 6): 1) Cape Jack, located in the southwest portion of St. Georges Bay was selected due to the close proximity of an active railroad to the eroding coastline; 2) Pomquet Beach, protected Natural Environment Park which has undergone a full dune migration between 1971 and 2007 and is and home to the endangered Piping Plover shorebird; 3) Dunns Beach, a previously studied area for which baseline erosion measurements were established by the Department of Natural Resources (Utting and Gallacher, 2008). The pre-1971 photos were found to be a challenge to orthorectify because common features used as control points within the 2007 base orthophotos have changed significantly, making accurate control point selection difficult. In addition, once orthorectified shore-line position was difficult to determine within the black and white imagery. As a result of the experience gained analysing the detailed areas, emphasis was placed on the analysis of the 1971 to 2007 orthophotos for the entire shoreline.

Figure 6 Location of regions of interest for detailed coastline change detection analysis.

3 Results

3.1 LiDAR

After the corrections for a heading shift were applied (heading shift = 0.18) to the dataset, inter-flight line misalignments were minimized. The ground returns were used to construct a TIN (triangulated irregular network) and a 1 m grid cell DEM was produced through linear interpolation of the (Fig. 7). A DSM (digital surface model) was also constructed in the same manner, but using ground and non-ground points, which incorporate features such as buildings and vegetation into the model.

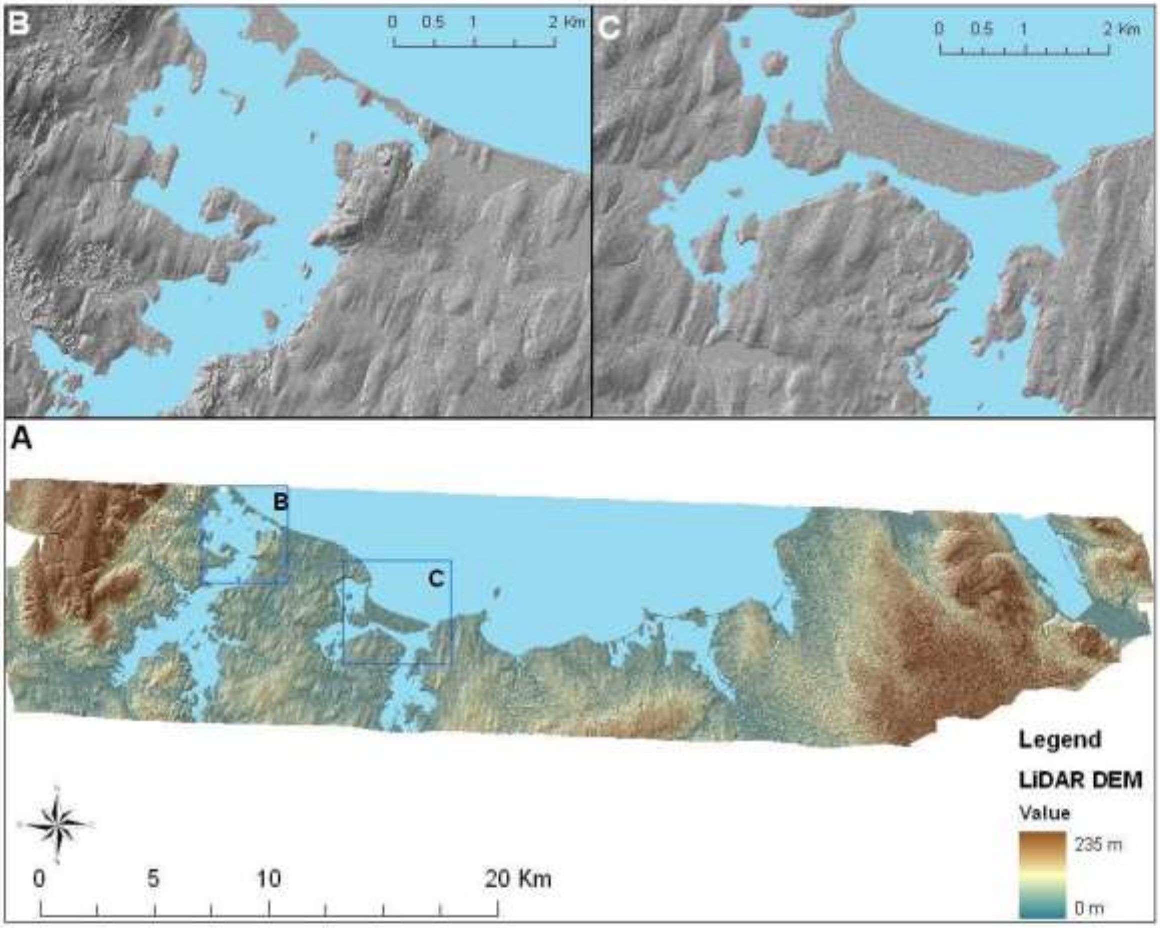

Figure 7: Colour shaded relief of the LiDAR derived DEM (A) showing two areas in detail ; greyscale hill shade Antigonish Harbour (B) and greyscale hill shade Pomquet Beach (C).

The DEM was validated using the acquired high precision RTK GPS survey data. The elevation differences between the LiDAR DEM and RTK GPS points were determined using the following equation: Δz = GPS – LiDAR DEM. Generally, the DEM elevations were matched well with the GPS data with an overall average difference of – 6 cm and a standard deviation of 15 cm (Fig. 8, 9).

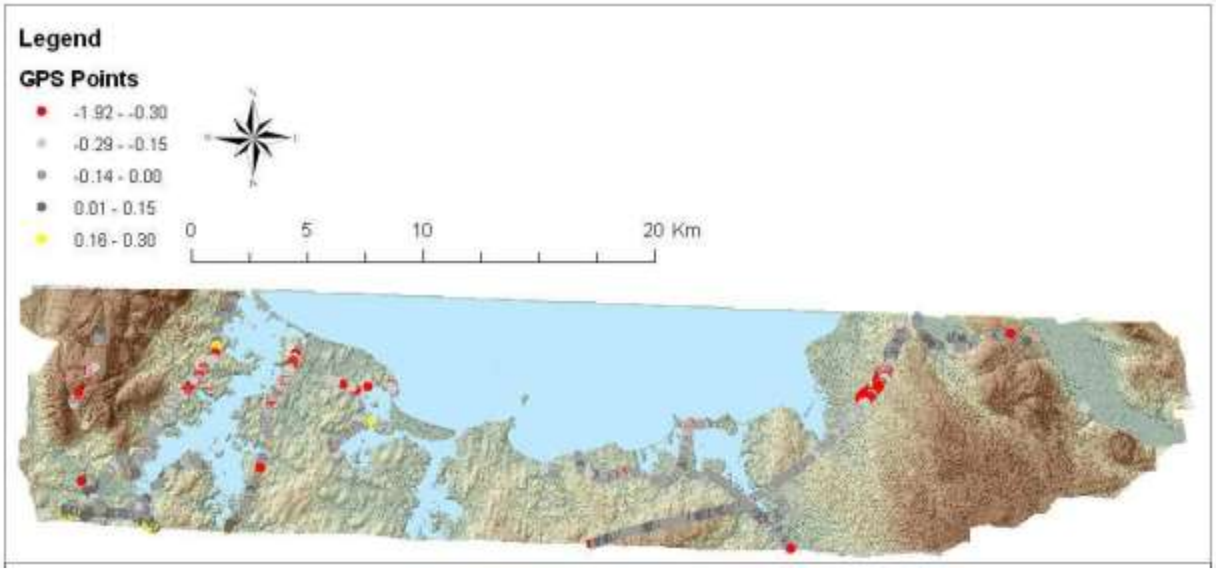

Figure 8: RTK GPS points over the LiDAR DEM. RTK GPS points are classified based on the difference in elevation (GPS-LiDAR). Points in grey are within 15 cm vertically and points in red and yellow are outside this range.

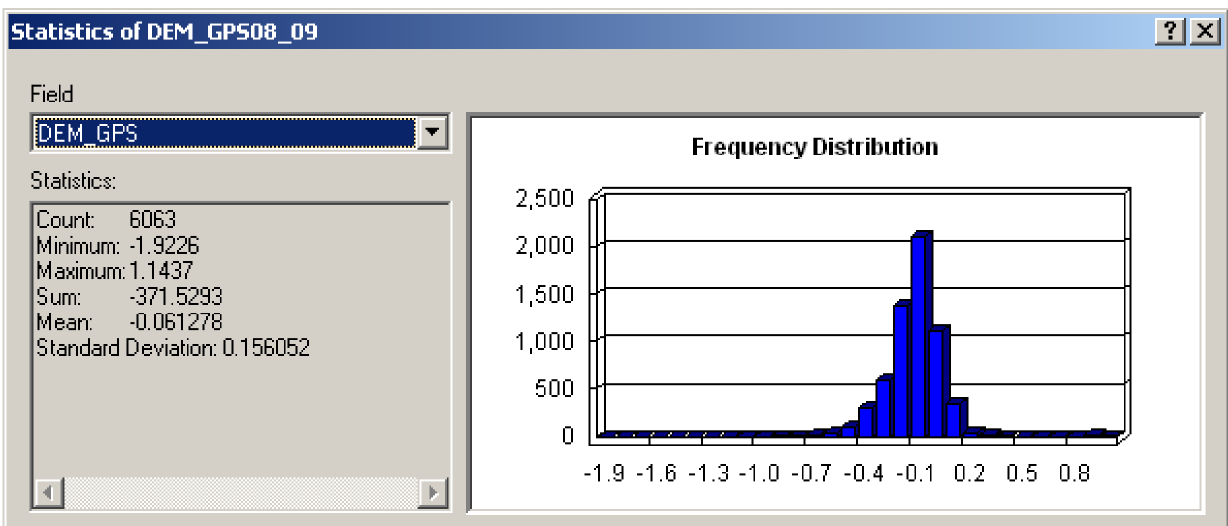

Figure 9: Summary statistics for the elevation difference between the RTK GPS points and the LiDAR DEM (Δz = GPS – LiDAR DEM).

3.2 Water Modeler

The Pictou tide gauge has the longest water level record on the Nova Scotia coast, was closest in proximity to Antigonish, and contains hourly records from 1970-1996. For these reasons, it was seen as a suitable gauge to establish tidal elevations for the Antigonish shoreline. Two water-level return period graphs were constructed from the water level time series. One graph was constructed for the current sea-level rise conditions (32 cm/century) and one incorporating was constructed for future sea-level rise conditions (70 cm/century). The 50-year return period flood level was ~1.95 m and the 100-year flood level was ~2.22 m) under the current sea-level rise conditions (Fig. 10). When future sea-level rise conditions were incorporated, the 50-year return period flood level increased to ~2.1 m and the 100-year return period flood level increased to ~2.5 m (Fig. 11, Table 1). Two cumulative probability graphs were constructed for the 2.27 m benchmark storm (December 30, 1993). The cumulative probability graph for current sea-level rise conditions indicated there was a 65% probability (represented by the black dot) of the event occurring within 23 years and a 99% probability that it would occur within 64 years (Fig. 12). With future sea-level rise conditions incorporated the probability of occurrence increased and the same event had a 65% probability of occurring within 19 years and a 99% probability of occurring within 45.5 years (Fig. 13, Table 2).

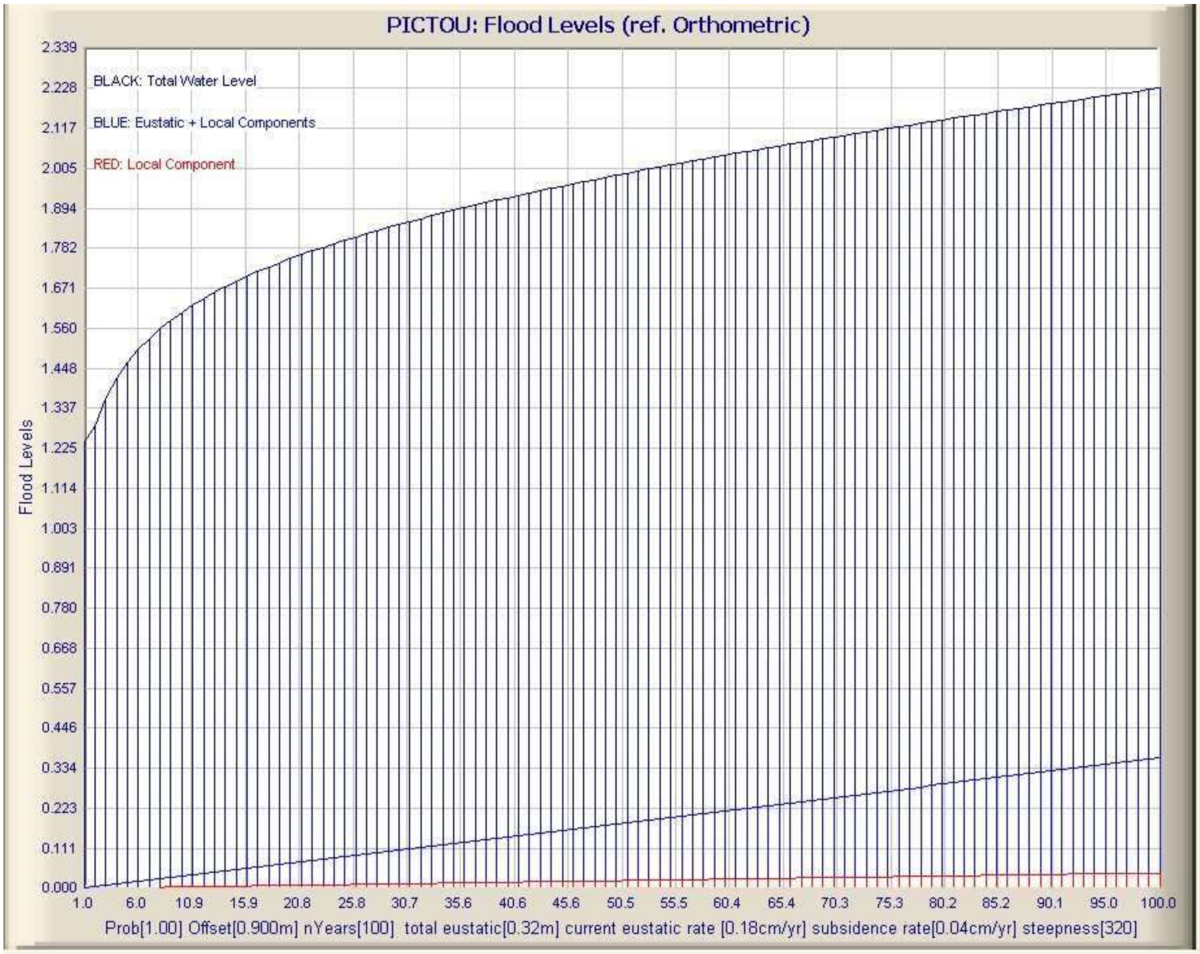

Figure 10: Water-level return periods for Pictou, Nova Scotia, using the observed sea-level rise rate of 32 cm/century.

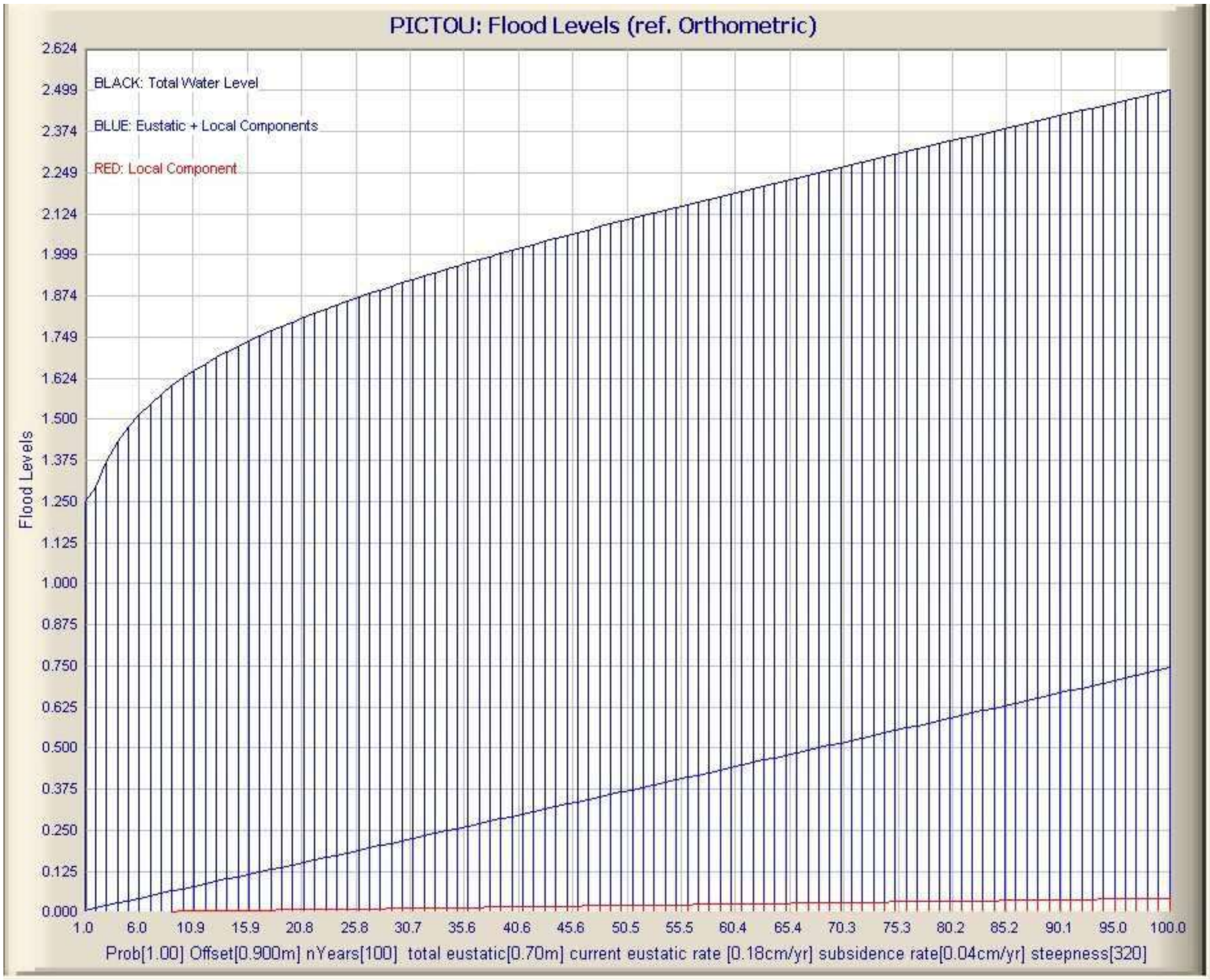

Figure 11: Water-level return periods for Pictou, Nova Scotia, using a future sea-level rise rate of 70 cm/century.

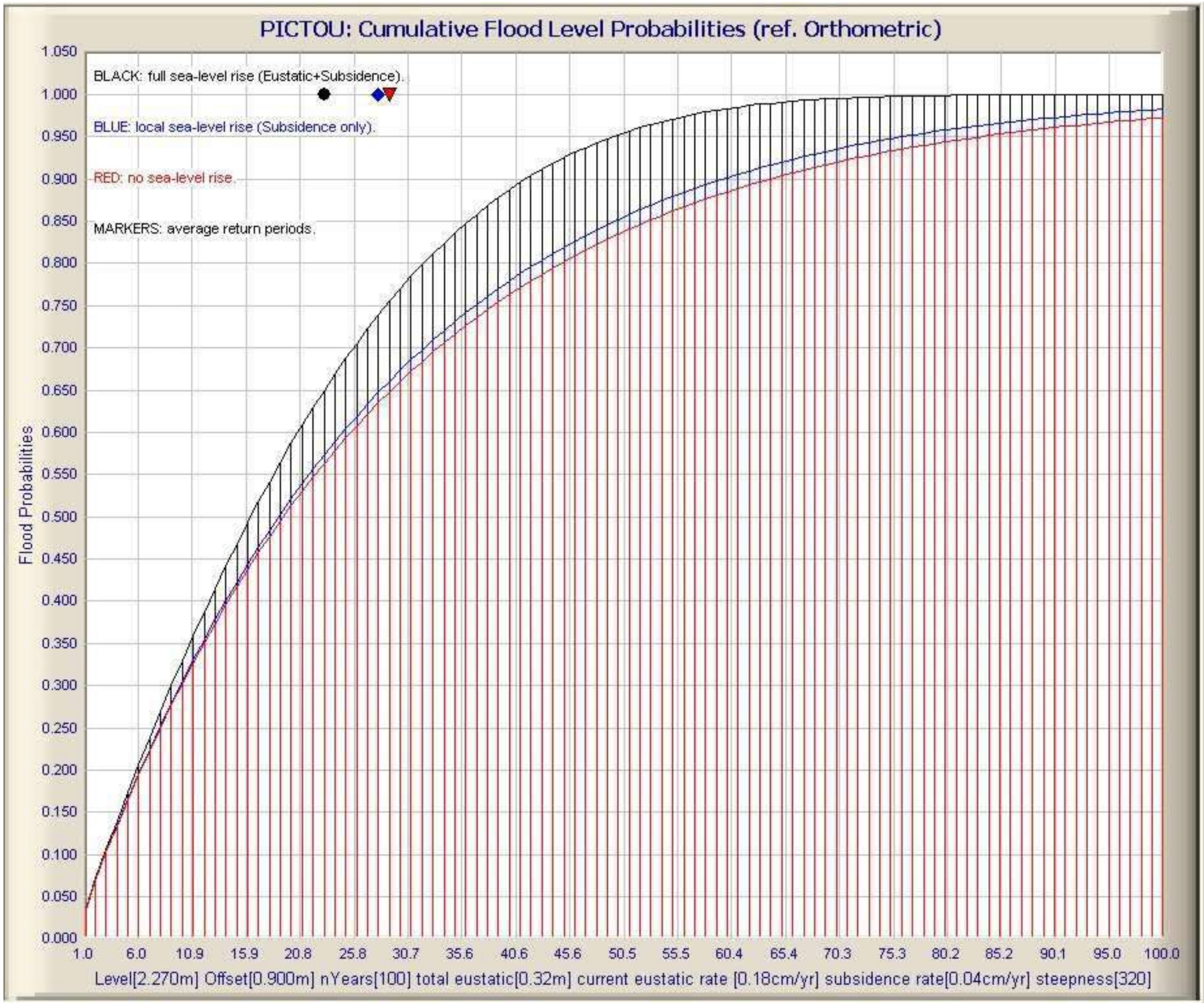

Figure 12: Cumulative flood-level probability graph for Pictou, Nova Scotia, using the current rate of sea-level rise (32 cm/century) for a 2.27 m flood (Dec 30, 1993 benchmark storm). The black dot represents the average expected return period of this water level (0.65 probability).

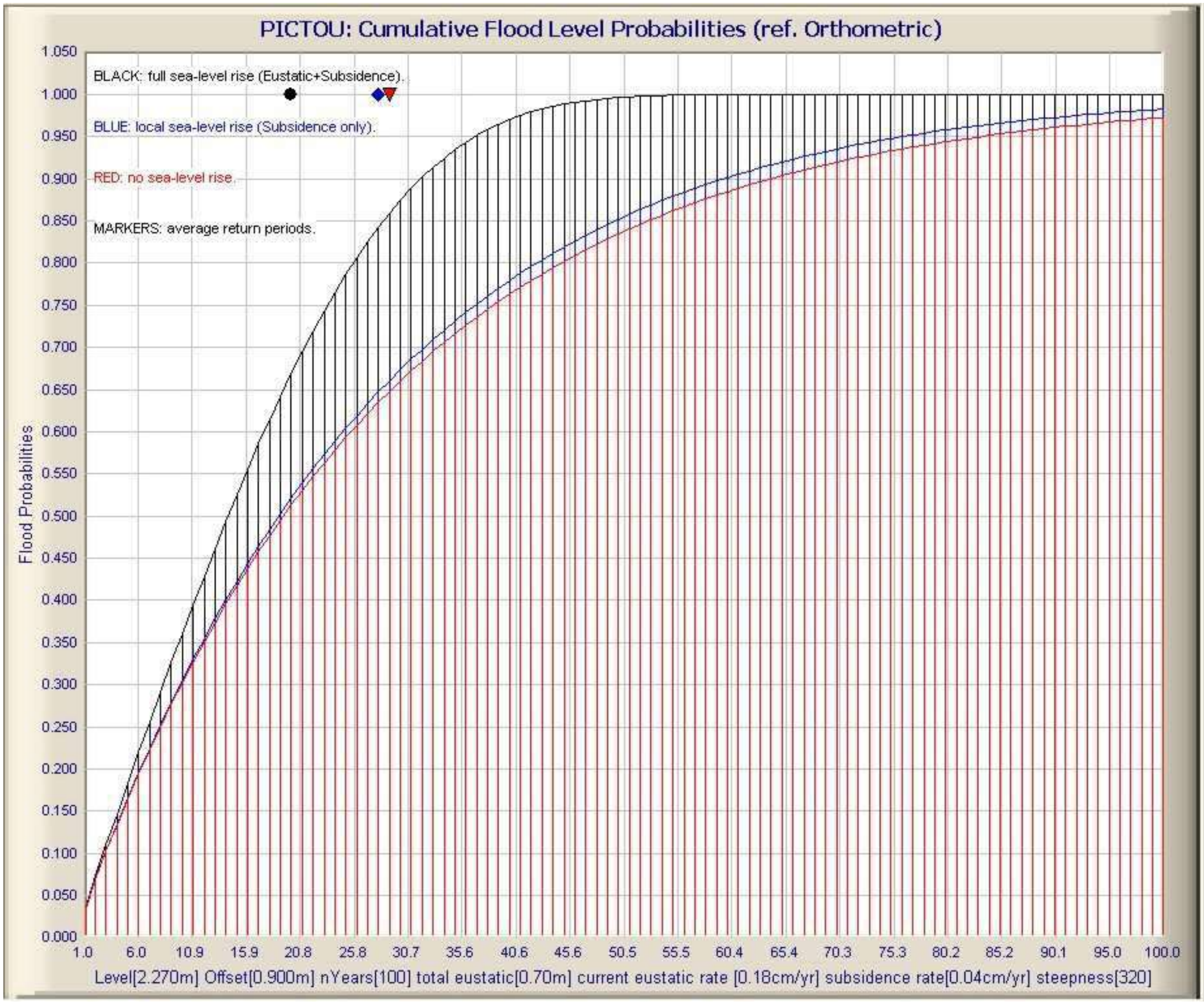

Figure 13: Cumulative flood-level probability graph for Pictou, Nova Scotia, using the future sea-level rise conditions (70 cm/century) for a 2.27 m flood (Dec 30, 1993 benchmark storm). The black dot represents the average expected return period of this water level (0.65 probability).

Table 1: Water levels for the 25, 50, 75, and 100 year return periods for different sea-level rise scenarios. Water levels above CGVD28.

Return Period (years)	RSL = 0.32 m/century (current rate)	RSL = 0.70 m/century (climate change)
25	~1.8 m	~1.85 m
50	~1.95 m	~2.1 m
75	~2.11 m	~2.3 m
100	~2.22 m	~2.5 m

Table 2: Cumulative probabilities for a 2.27 m flood (Dec. 1993) for different sea-level rise scenarios.

Cumulative Probability	RSL = 0.32 m/century (current rate)	RSL = 0.70 m/century (climate change)
0.65	23 years	19 years
0.75	28.5 years	23 years
0.95	49 years	36.5 years
0.99	64 years	45.4 years

3.3 Flood Risk Maps

Two inundation maps were constructed for the report. The first map represents two water levels symbolized by the 50-year and 100-year return period floods under the current sea-level rise conditions (1.95 m and 2.22 m flood levels respectively) (Fig. 14). The second map represents the December 1993 storm event projected 50 and 100 years into the future assuming a sea-level rise of 70 cm/century (2.27 m, 2.62 m, and 2.97 m flood levels respectively) (Fig. 15). Because so much of the shoreline in this region is protected from development by the Nova Scotia Department of Natural Resources, the area is not very populated and these water levels do not have a large impact on infrastructure. If a 1.95 m flood were to occur, then 2 buildings would be affected based on the existing mapping. However, if a 2.97 m flood were to occur, 21 buildings become affected (Table 3). These maps are just an example for some past storm-surge events and return period values. Although this report presents two flood maps, all of the modelled flood levels have been delivered on DVD to the clients, who may map any desired level.

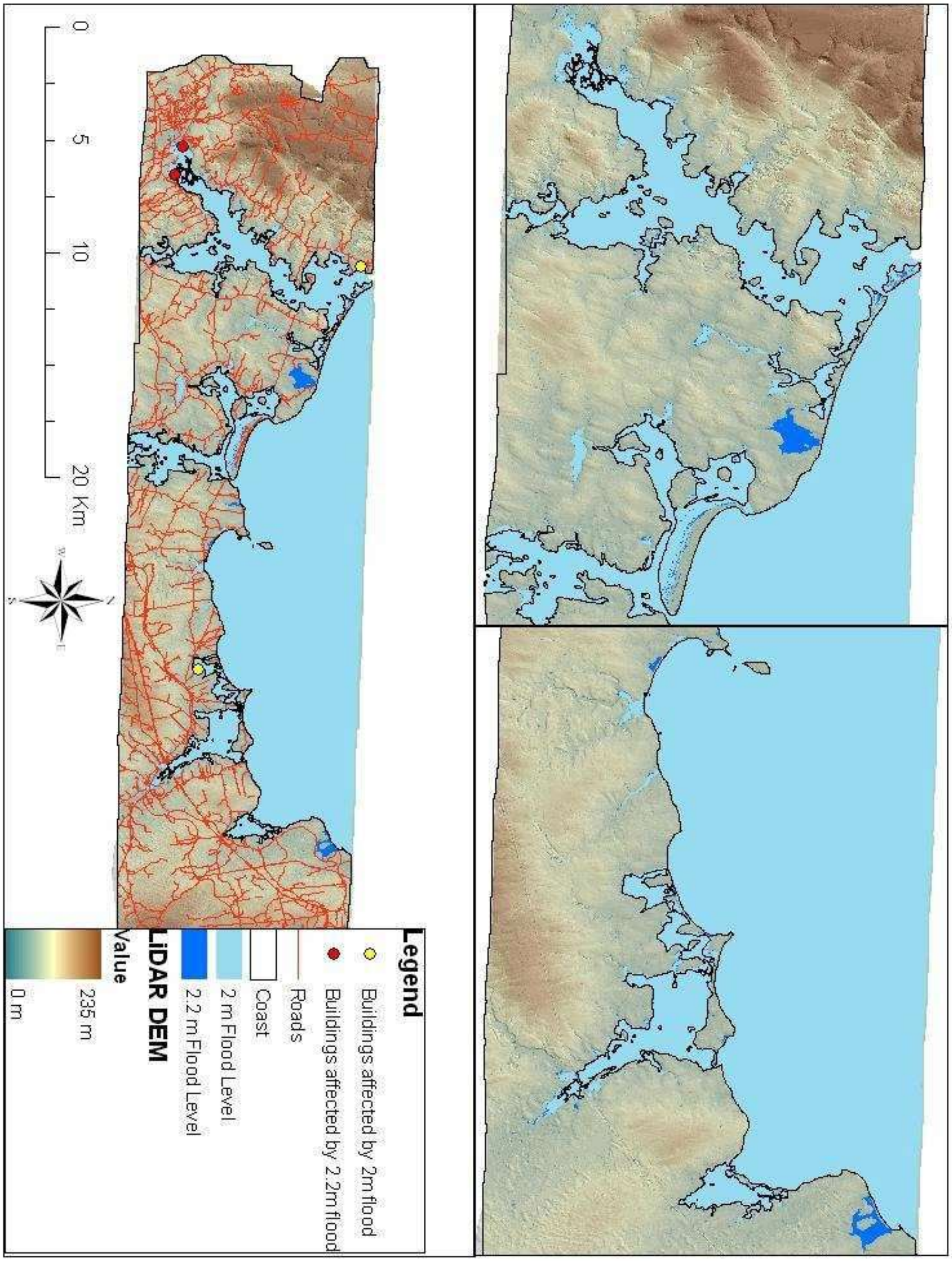

Figure 14: Flood inundation map showing the 50-year and 100-year return period water levels under current sea-level rise conditions (32 cm/century). The black outline depicts the current shoreline position.

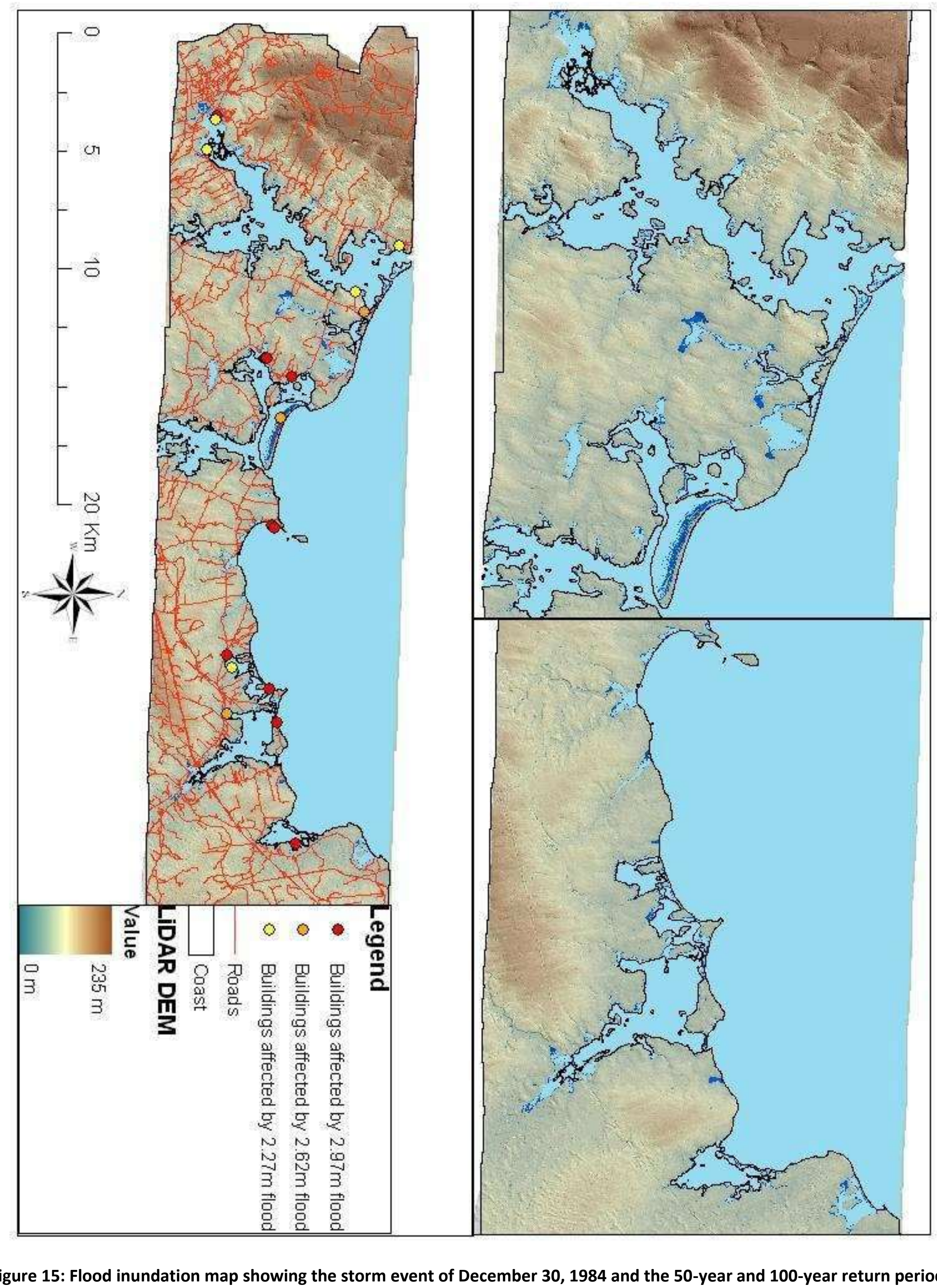

Figure 15: Flood inundation map showing the storm event of December 30, 1984 and the 50-year and 100-year return period water levels under normal sea-level rise conditions (70 cm/century superimposed on the storm event). The black outline depicts the current shoreline position.

Table 3: Infrastructure affected by various flood levels.

Flood Level	Units of infrastructure affected
1.95 m	2
2.22 m	4
2.27 m	5
2.62 m	9
2.97 m	21

3.4 Coastline change detection (erosion and accretion)

The results of the detailed coastline change detection have shown that the coastline has variable rates of change based on the composition and local relief of the material. For example, Cape Jack has undergone an average rate of erosion of 22 cm/year where the till bank forms the coastline and has retreated on an average 2.1 m between 1954 and 2007 (Fig. 16). In contrast, an area to the east where the coastline is comprised of a gravel bar with a pond landward has undergone an average rate of erosion of 71 cm/year where the till bank forms the coastline and has retreated on average 6.7 m between 1954 and 2007 (Fig. 16). In both cases the rail line is directly landward of the coastline and is vulnerable to continued erosion.

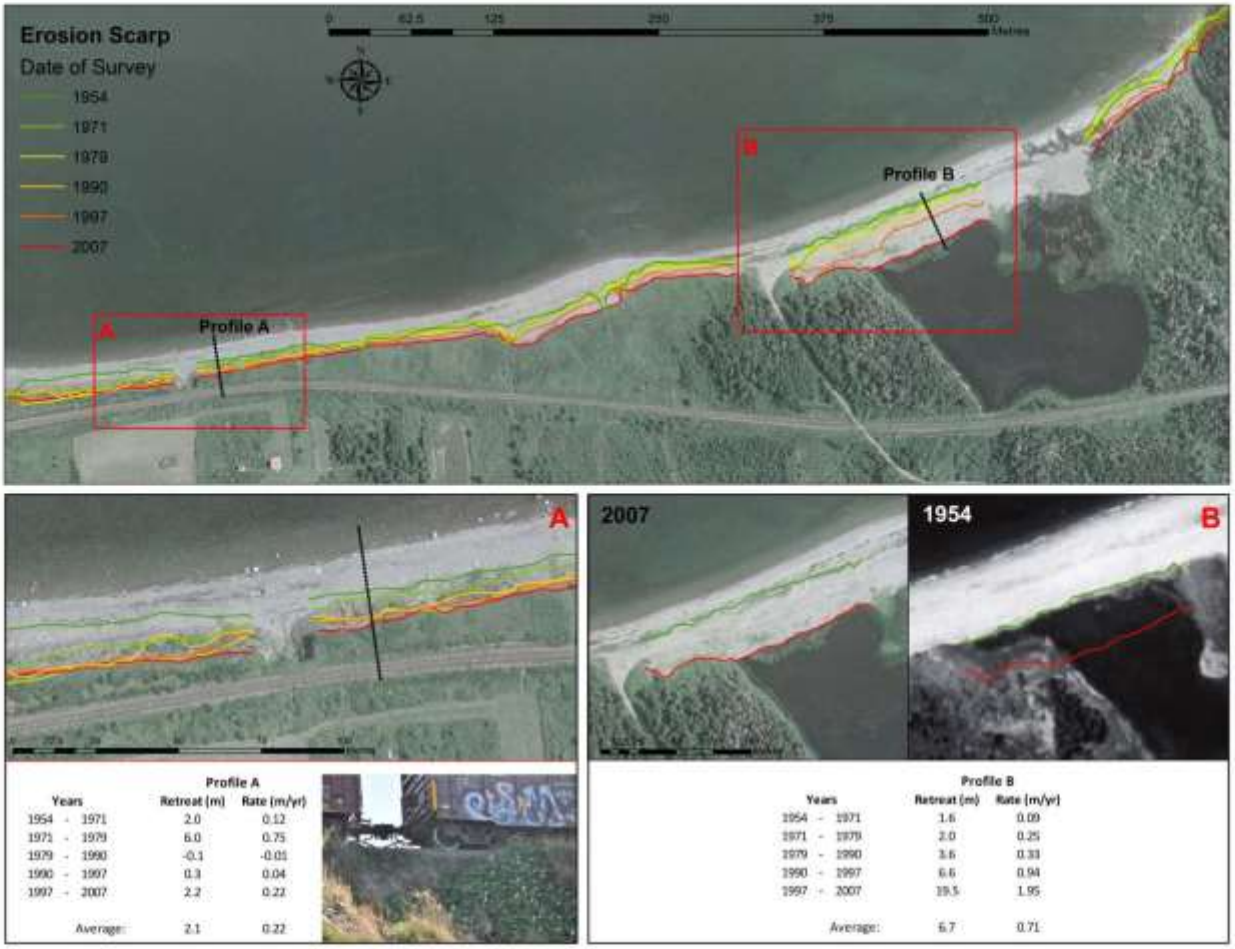

Profile A Years	Retreat (m)	Rate (m/yr)
1954 - 1971	2.0	0.12
1971 - 1979	6.0	0.75
1979 - 1990	-0.1	-0.01
1990 - 1997	0.3	0.04
1997 - 2007	2.2	0.22
Average:	2.1	0.22

Profile B Years	Retreat (m)	Rate (m/yr)
1954 - 1971	1.6	0.09
1971 - 1979	2.0	0.25
1979 - 1990	3.6	0.33
1990 - 1997	6.6	0.94
1997 - 2007	19.5	1.95
Average:	6.7	0.71

Figure 16: Cape Jack detailed coastline change detection. Photos range in time from 1954 to 2007. This section of coastline has experienced variable rates of erosion as demonstrated by profile A and B.

Variable rates of change have also been observed along a stretch of an eroding drumlin in the Dunns Beach area. The western portion of the drumlin has eroded at a rate of 60 cm/year between 1954 and 2007. In contrast, the eastern extent has undergone a much lower average retreat of 26 cm/year during the same time period. The maximum retreat occurred between 1971 and 1979, and averaged 10.4 m of erosion in the west and 4.0 m of erosion in the east. The area was found to be highly variable in observed rates of erosion along the western to eastern extent over temporally spaced surveys. This may be related to the nature of slumping in the area and the dominant wave pattern (Fig. 17).

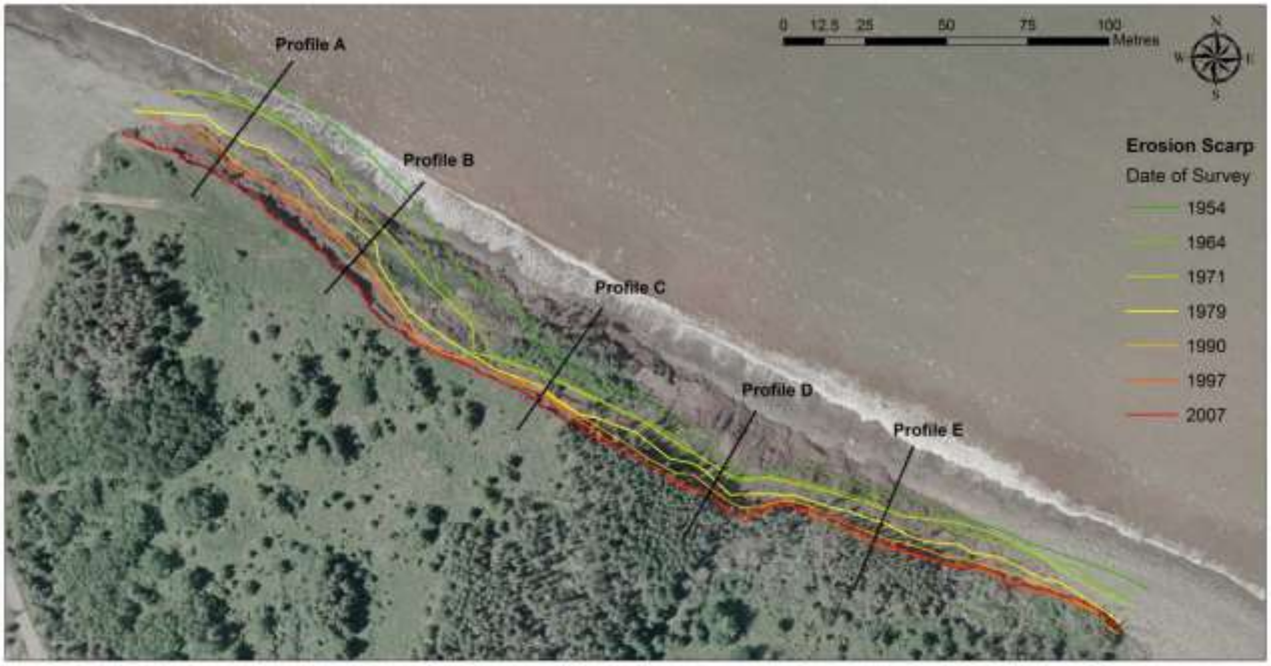

Scarp Retreat: Dunns Beach

Years	Profile A Retreat (m)	Profile A Rate (m/yr)	Profile B Retreat (m)	Profile B Rate (m/yr)	Profile C Retreat (m)	Profile C Rate (m/yr)	Profile D Retreat (m)	Profile D Rate (m/yr)	Profile E Retreat (m)	Profile E Rate (m/yr)
1954 - 1964	8.5	0.85	5.9	0.59	5.2	0.52	3.0	0.30	4.7	0.47
1964 - 1971	1.4	0.20	7.1	1.01	0.6	0.09	0.3	0.04	0.5	0.07
1971 - 1979	10.4	1.30	4.4	0.55	4.3	0.54	3.8	0.48	3.9	0.49
1979 - 1990	5.1	0.46	6	0.55	1.1	0.10	2.6	0.24	4.3	0.39
1990 - 1997	1.7	0.24	1.2	0.17	0.3	0.04	2.0	0.29	2.8	0.40
1997 - 2007	5.6	0.56	6.5	0.65	2.7	0.27	0.3	0.03	-1.1	-0.11
Average:	5.5	0.60	5.2	0.59	2.4	0.26	2.0	0.23	2.5	0.28

Figure 17: Coastline change detection of Dunn's beach. Photos range in time from 1954 to 2007. This section of coastline has experienced variable rates of erosion from 23 cm/year to 60 cm/year as demonstrated by profiles A to E.

In contrast to the observed eroding coastline, an area of Pomquet Beach was observed to prograde between 1971 and 2007 resulting in the addition of a dune formation. Profiles showed the extent of this sea-ward dune migration to range between 17.8 m in the west and 43.4 m in the east (Fig. 18). This is interpreted to be a result of the long-shore drift and sediment transport.

The role of vegetation and drainage is considered to be important in all environments of unconsolidated sediments and will be the focus of continued research into coastline change.

Figure 18 Pomquet Beach detailed coastline change detection. Photos range in time from 1971 to 2007. Coastline in this area has undergone a seaward dune migration over the surveyed dates.

4 Discussion

Based on previous studies performed in the Maritime region concerning flood inundation analysis, it has been determined that LiDAR derived DEM's are suitable for flood risk mapping as they are accurate enough to represent storm surges of 1-2 m in magnitude and map the long term effects of decimetre to metre ranges of climate change induced sea-level rise. However, it is imperative that detailed ground validation, such as GPS surveys, are carried out to ensure that the LiDAR data is of adequate specifications to facilitate reliable results (Webster et al. 2004). It is unfortunate that the LiDAR survey conducted in this area had calibration issues that took months to resolve and did not allow for extensive work on the flood risk mapping component. For example, a detailed analysis of adaptation and mitigation steps could be the next step in the analysis. The LiDAR data were repaired however and have provided the accuracy required to generate flood risk maps.

Water Modeler has been tested in only a few different cases, and has been demonstrated to be a useful method for providing the risks associated with coastal flooding and storm-surge events (Webster et al. 2008). The work by Bernier (2005) and Thompson et al. (2009) have been compared for the Pictou tide gauge. Thompson et al. (2009) have calculated the 100 year return period of the total water level for this site to be approximately 2.3 m. using Water Modeler for the Pictou tide gauge we have estimated the 100 year return period total water level to be 2.2 m. Antigonish only had tide gauge records from 1950-1951, which is not a long enough time series to perform any predictions for return periods with confidence, plus this was prior to the construction of the Cape Breton causeway. When examining the water levels in the Pictou tide gauge record, residuals were calculated (predicted water level – observed = residual) to determine storm surges. Since Charlottetown is across the Northumberland Strait most storm surges that affected Pictou, also were observed in Charlottetown. Thus any high water levels from storm surges observed in Pictou were compared to Charlottetown. However, there was an anomaly with the tide gauge data for Pictou for a storm event at the Pictou tide gauge (2.15 m on December 30, 1984) that was not observed at Charlottetown and there was no storm event recorded by Environment Canada. This event is still under investigation, but was not used as a benchmark storm event for modelling.

5 Conclusions

Flood inundation mapping allows for the observation of at-risk areas from flooding and storm-surge events and allows for future planning within these sensitive areas. Since this is the first time the Antigonish county shoreline has been analyzed for flood and erosion risk with LiDAR and a temporal series of orthophotos, this work can act as the basis for future planning and research activities. The flood risk maps were generated in such a way that as new sea-level rise projections are proposed, the appropriate water flood level can be extracted and examined. The erosion study has highlighted how a systematic approach to the entire coastline is required as a result of the variable composition, relief and orientation affects the level of resistance to erosion. Our work on erosion provides the base for future studies taking into account some of the controlling factors such as composition and orientation. The use of Geomatics tools, such as a LiDAR DEM, Water Modeler, and a time series of orthophotos can become valuable tools for coastal communities to better plan for the future.

Acknowledgments

We would like to thank several individuals for their assistance during this project; Chris Hopkinson, Allyson Fox, Suzanne Monette and James from the Applied Geomatics Research Group. Garth Demont and Dan Utting of DNR for their assistance in the field and acquiring aerial photographs. Donnie Cameron of NS Economic Development and Will Green of NS Environment for funding and Ray MacIsaac of Department of Fisheries and Oceans for indirect funding support.

References

Bernier, N.B. (2005) Annual and seasonal extreme sea levels in the Northwest Atlantic: hindcasts over the last 40 years and projections for the next century. PhD thesis, Dalhousie University.

Bernier, N.B., Thompson, K.R. (2006) Predicting the frequency of storm surges and extreme sea levels in the Northwest Atlantic. J Geophys Res 111:10009. doi:10.1029/2005JC003168.

Church, J., & Gregory, J. (2001). Changes in Sea Level. In Climate Change 2001: The Scientific Basis: Contribution of working Group 1 to the Third Assessment Report of the Intergovernmental Panel on Climate Change (pp. 639-692). Cambridge, New York: Cambridge University Press.

Flood, M., and Gutelius, B. (1997). Commercial Implications of Topographic Terrain Mapping Using Scanning Airborne Laser RaDAR. Photogrammetric Engineering and Remote Sensing , 4, 327-366.

Forbes, D.L., Manson, G.K., Charles, J., Thompson, K.R., and Taylor, R.B. (2009). Halifax Harbour Extreme Water levels in the Context of Climate Change: Scenarios for a 100-Year Planning Haorizon. Geological Survey of Canada, Open File 6346, 21 p.

IPCC, 2007: Climate Change 2007: The Physical Science Basis. Contribution of Working Group I to the Fourth Assessment Report of the Intergovernmental Panel on Climate Change [Solomon, S., D. Qin, M. Manning, Z. Chen, M. Marquis, K.B. Averyt, M. Tignor and H.L. Miller (eds.)]. Cambridge University Press, Cambridge, United Kingdom and New York, NY, USA, 996 pp.

Liu, X. (2008). Airborne LiDAR for DEM Generation: Some Critical Issues. Progress in Physical Geography , 32 (1), 31-49.

MacCaulay, P. (2009). Canadian Hydrographic Services (CHS). Personal Communication.

Meehl, G.A., T.F. Stocker, W.D. Collins, P. Friedlingstein, A.T. Gaye, J.M. Gregory, A. Kitoh, R. Knutti, J.M. Murphy, A. Noda, S.C.B. Raper, I.G. Watterson, A.J. Weaver and Z.-C. Zhao, (2007). Global Climate Projections. In: Climate Change 2007: The Physical Science Basis. Contribution of Working Group I to the Fourth Assessment Report of the Intergovernmental Panel on Climate Change [Solomon, S., D. Qin, M. Manning, Z. Chen, M. Marquis, K.B. Averyt, M. Tignor and H.L. Miller (eds.)]. Cambridge University Press, Cambridge, United Kingdom and New York, NY, USA.

Nicol, A. (2006). Planning for coastal Areas in the context of changing climate conditions in Antigonish County. Unpublished report. Independent project PLAN 6000. Dalhousie University, December 2006.

Raper, S. C., & Braithwaite, R. J. (2006). Low Sea Level Rise Projections from Mountain Glaciers and Icecaps Under Global Warming. Nature , 439, 311-313.

Shaw, J., Taylor, R., Forbes, D., Ruz, M., & Solomon, S. (1998). Sensitivity of the Coasts of Canada to Sea-level Rise. Geological Survey of Canada (Bulletin 505), Natural Resources Canada , 1-79.

Thompson, K.R., Bernier, N.B. and Chan, P. (2009). Extreme sea levels, coastal flooding and climate change with a focus on Atlantic Canada. Natural Hazards. No. 51, pp. 139-150.

Titus, J. G., Park, R. A., Leatherman, S. P., Weggel, J. R., Greene, M. S., Mausel, P. W., et al. (1991). Greenhouse Effect and Sea Level Rise: The Cost of Holding Back the Sea. Coastal Management , 19, 171-204.

Utting, D. J. and Gallacher, A. F. (2009): Coastal Environment and Erosion in Southwest St. Georges Bay, Antigonish County. In Mineral Resources Branch, Report of Activities 2008; Nova Scotia Department of Natural Resources, Report ME 2009-1, p. 139-149.

Webster, T., Mosher, R., & Pearson, M. (2008). Water Modeler: A Component of a Coastal Zone Decision Support System to Generate Flood-risk Maps from Storm-surge Events and Sea-level rise. Geomatica, 62 (4), 257-265.

Webster, T. and Stiff, D. (2008). The prediction and mapping of coastal flood risk associated with storm surge events and long-term sea level changes. In Risk Analysis VI Simulations and Hazard Mitigation. WIT Press. Edited by Brebbia, C.A. and Beriatos, E. pp. 129-139.

Webster, T., & Dias, G. (2006). An Automated GIS Procedure for Comparing GPS and Proximal LiDAR Elevations. Computers & Geosciences , 32, 713-726.

Webster, T.L, Forbes, MacKinnon, E., and Roberts, D. (2006). Chapter 4.4 LiDAR digital elevation models and flood-risk mapping. Environment Canada report: Daigle, R. and Project Research Team. 2006. Impacts of sea level rise and climate change on the coastal zone of southeastern New Brunswick/ Impacts de l'élévation du niveau de la mer et du changement climatique sur la zone côtière du sud-est du Nouveau-Brunswick. Environment Canada, 611 pp. (also on CD-ROM and on-line at http://atlantic-web1.ns.ec.gc.ca/slr/).Webster, T., Forbes, D., MacKinnon, E., & Roberts, D. (2006). Flood-risk Mapping for Storm-surge Events and Sea-level Rise Using LiDAR for Southeast New Brunswick. Canadian Journal of Remote Sensing , 32 (2), 194-211.

Webster, T., & Forbes, D. (2005). Using Airborne LiDAR to Map Exposure of Coastal Areas in Maritime Canada to Flooding from Storm-surge Events: A Review of Recent Experience. Canadian Coastal Conference (pp. 1-11). LiDAR Surveys for Storm-surge Flooding.

Webster, T.L. (2005). LIDAR validation using GIS: A case study comparison between two LIDAR collection methods. GeoCarto International. Vol. 20, No. 4, pp. 11-19.

Webster, T., Forbes, D., Dickie, S., & Shreenan, R. (2004). Using Topographic LiDAR to Map Risk from Storm-surge Events for Charlottetown, Prince Edward Island, Canada. Canadian Journal of Remote Sensing , 30 (1), 64-76.

Webster, T.L, Forbes, D.L, Dickie, S., Colvill, R., and Parkes, G., (2002). Airborne Imaging, Digital Elevation Models and Flood Maps. Supporting Document number 4. In Coastal impacts of Sea-Level Rise on Prince Edward Island. Edited by Forbes D.L. Climate Change Action Fund Project A041. Geological Survey of Canada Open File 4261.

Wehr, A., & Lohr, U. (1999). Airborne Laser Scanning - An Introduction and Overview. Journal of Photogrammetry and Remote Sensing , 54, 68-82.